ISBN: 978-628-96613-3-0. ISSN: 2414-6390. Digital Object Identifier: https://dx.doi.org/10.18687/LACCEI2026.1.1.1750

LoRa-based IoT System for Particulate Matter (PM) Monitoring in San Jerónimo, Cusco, Peru

Willy Huallpa Pillco[1]; Darwin Auccapuri Quispetupa[2]
[1,2]*Pontificia Universidad Catolica del Perú, Perú, willy.huallpa@pucp.edu.pe, dauccapuri@pucp.edu.pe*

Abstract– The district of San Jerónimo in Cusco, Peru, faces a critical environmental problem due to emissions from artisanal brick kilns and the lack of continuous air quality monitoring. This work presents the design and validation of a low-cost IoT sensor network based on LoRa technology for monitoring PM2.5 and PM10 in areas affected by these activities. The architecture integrates solar-powered ESP32 sensor nodes with an industrial XDB1002-11 sensor (Modbus-RTU), a LoRa gateway, and a cloud platform on Google Cloud, using InfluxDB and Grafana for time-series storage and near real-time visualization. Field tests in a semi-urban environment confirmed stable links up to 2.39 km in the 915–928 MHz band and, after link-level optimizations, a global effective Packet Delivery Ratio of 92.3% and a real PDR of 84.6%. The photovoltaic subsystem provided 14–30 h of autonomy, while highlighting opportunities to improve energy management. Measurements revealed PM10 and PM2.5 peaks above 800 µg/m³ and 300 µg/m³ near the kilns, far exceeding WHO guidelines and evidencing their impact on surrounding urban areas. The results demonstrate the feasibility and potential of the proposed solution to support municipal air-quality management in rural and semi-urban settings.

Keywords-- IOT, LoRa, PM2.5, PM10, Cusco.

I. Introduction

Air pollution represents one of the greatest challenges for public health in rapidly growing urban areas. Consequently, the World Health Organization (WHO) emphasizes the importance of monitoring suspended particles such as PM10 and PM2.5, which can penetrate deep into the lungs and enter the bloodstream, leading to chronic diseases and premature mortality. This monitoring process enables the establishment of preventive alerts and the design of emission control policies that directly contribute to human life protection [1].

In the case of Peru, air quality monitoring becomes a pillar for decision-making in public environmental management, since it allows risks to be identified and mitigated in urban centers such as the city of Cusco, located in the south-central area of the country. According to Wharton [2], peak values of up to 153 µg/m³ for PM2.5 and 142 µg/m³ for PM10 were obtained, values that exceed the levels established by Governmental Organizations in the country as stipulated by the Ministry of the Environment. [3].

This situation increases the respiratory vulnerability of the population and accelerates the degradation of cultural heritage due to the deposition of soot generated by the kilns used in brick and tile manufacturing in the San Jerónimo district, one of the most important in the city of Cusco. Artisanal brick kilns produce a strong environmental and health impact as a consequence of the use of low-quality fuels and inefficient ovens that emit large quantities of smoke, soot, and fine particulate matter. This pollution deteriorates air quality in the influenced areas and continuously exposes workers and neighboring populations. In that context, measuring PM10 and PM2.5 at the brick kilns is key to dimensioning the problem and supporting the need for control actions.

Although spot studies have evidenced the magnitude of the environmental and social impact, the lack of continuous monitoring systems still limits local authorities' ability to design evidence-based public policies. Traditional reference stations, although highly accurate, are costly, complex to maintain, and not easily scalable, which hinders their implementation by local governments with limited resources.

This technological gap creates a void in available environmental information and, consequently, in the capacity to respond to pollution. In this context, IoT solutions and low-power wide-area networks (LPWAN), in particular those using LoRa, consolidate as a viable alternative that is low-power and low-cost, enabling the deployment of robust, scalable environmental monitoring IoT networks that operate in near real time. [4] [5] These technologies make it possible to deploy low-cost sensor networks that cover extensive areas with minimal energy consumption, promoting sustainability and reducing initial investment. Moreover, the IoT architecture enables wireless transmission of data almost in real time to cloud platforms where the information is processed, visualized, and shared with authorities and citizens.

This work designs, implements, and validates a low-cost IoT system for air quality monitoring in areas influenced by the brick kilns of San Jerónimo, based on a scalable architecture with PM2.5 and PM10 sensor nodes, a LoRa gateway, and a cloud platform aimed at democratizing access to environmental information and strengthening local management.

II. Methodology

The methodological process for the design and implementation of the wireless sensor network for monitoring particulate matter PM2.5 and PM10 was structured as follows:

a) *Site selection:* Identification of the area of influence where brick factories have impact (see Fig. 1). This supports the delimitation of the communication architecture.

Fig.1 Location of factories – San Jerónimo District, Cusco. Adapted from [6].

b) *Identification and validation of technical aspects such as (see Fig. 2):*
   - Data acquisition: Integration of PM1, PM2.5 and PM10 sensors with embedded systems using LoRa technology configured for periodic measurement.
   - Transmission: Focused mainly on the wireless transmission of data obtained from the sensors, as well as the network architecture.
   - Power: Priority is given to autonomous power with solar panels, batteries, and controllers sized according to consumption and radiation.
   - Housing: Physical protection through enclosures resistant to dust, humidity, and rainfall.
   - Data visualization: Validation of wireless data transmission, storage, and presentation of data in real-time dashboards.

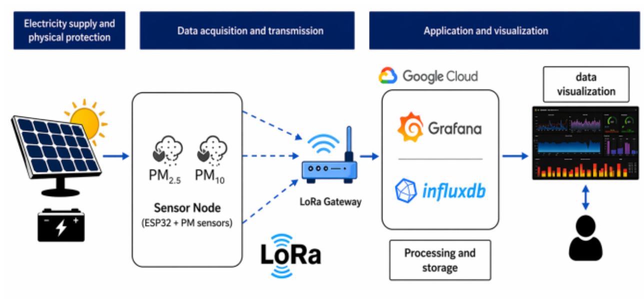

Fig.2 Elements of the proposed particulate matter monitoring system.

c) *Testing and assembly.*

d) *Field implementation and validation of data transmission and visualization.*

III. IMPLEMENTATION PROCESS

To achieve the project objective, it was organized into four main subsystems as follows:

a) *Data Acquisition Subsystem or Perception Layer:* This is composed of the sensor nodes, which operate autonomously and are responsible for acquiring measurements of environmental variables (PM2.5, PM10).

This perception process required hardware integration, differentiating two main devices: the sensor node and the gateway node. See Fig. 3.

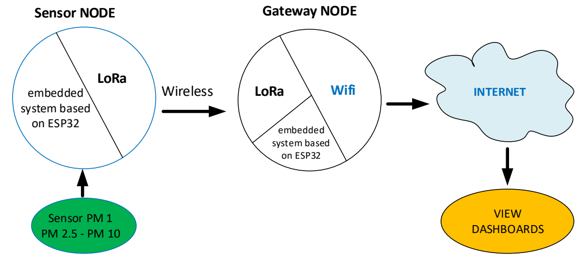

Fig.3 Sensor Node and Gateway Node

On the one hand, for the sensor node the LilyGO LoRa32 SX1276 module (based on ESP32) was chosen as the processing core because it integrates both the LoRa radio and a low-power, high-performance microcontroller unit (MCU). Unlike technologies such as Zigbee or XBee, which require a complementary MCU typically included in an additional module, this integration in the LilyGO solution reduces system complexity and minimizes possible points of failure during the integration process. On the other hand, study [7], which compares the performance of ZigBee and LoRa for energy and environmental monitoring in buildings, shows a clear advantage of LoRa in terms of penetration through cement and concrete walls, as well as range in the presence of obstacles. These results anticipate better LoRa performance in a complex and dense urban environment such as the San Jerónimo district, where transmission over several hundred meters is required in the presence of buildings.

For particulate matter measurement, the industrial sensor XDB1002-11 was used, which employs the laser scattering principle to measure particle concentrations (0–1000 µg/m³) and transmits data via RS-485 under the Modbus-RTU protocol. To ensure communication between the sensor and the microcontroller (LILYGO LoRa), a MAX485 converter module is managed. Connections can be observed in Fig. 4, and Fig.5.

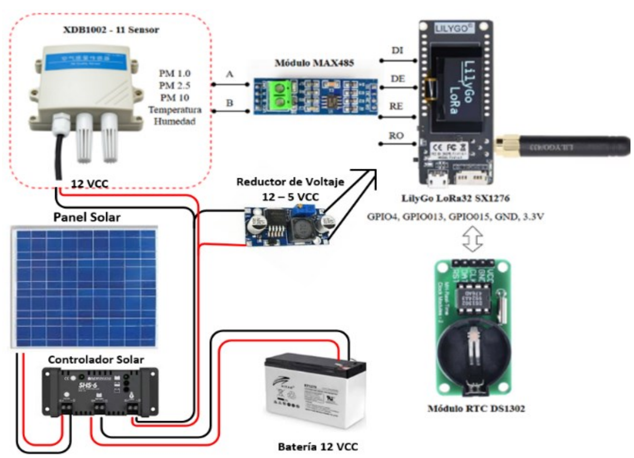

Fig.4 Sensor Node diagram.

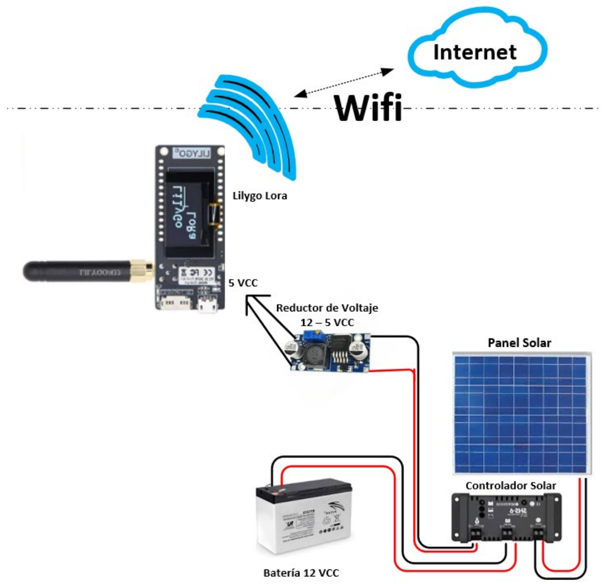

Fig.5 Gateway Node diagram.

Regarding the Gateway Node, this central device uses a TTGO T-Beam V1.2 development module, which integrates a LoRa SX1276 transceiver and Wi-Fi connectivity, as shown in Fig. 3. The gateway operates in an active listening mode to intercept node frames, verify data integrity (CRC), and encapsulate the payload in JSON format for sending to the cloud. This configuration is only necessary for the Gateway Node, while the Sensor Node does not require it. Likewise, Table I summarizes the characteristics of each node.

TABLE I
SENSOR AND GATEWAY NODE

Characteristic	Sensor Node	Gateway Node
Main module	LilyGO LoRa32 SX1276 (ESP32 + LoRa), Voltage: 5 VDC	LilyGO LoRa32 SX1276 (ESP32 + LoRa) Voltaje: 5 VDC
Funtion	Measures and sends PM concentrations via LoRa	Receives and forwards sensor data to the cloud
Sensor	XDB1002-11 (laser scattering, RS-485 Modbus) Voltage: 12 VDC Margin of error: ≤ 1.1% (typical systematic error), expanded uncertainty 14.2% (k = 2) [8]	Not required
Internet connection	Not required	Required
RTC (R.Time clock)	Required	Required

b) Telecommunications subsystem: The implemented topology corresponds to a point-to-multipoint (P2MP) or star configuration, in which two sensor nodes and one gateway node are used. Half-duplex communication is employed. Sensor node (far) is located within the influence area of the brick kilns (see Fig.1), while sensor node (near) is installed outside that area to compare and analyze measurement behavior under different environmental conditions. The operating frequency is within the range permitted in Peru (915–928 MHz), compatible with the LilyGO LoRa32 SX1276 module used. Fig.6 shows the proposed network topology used in the tests.

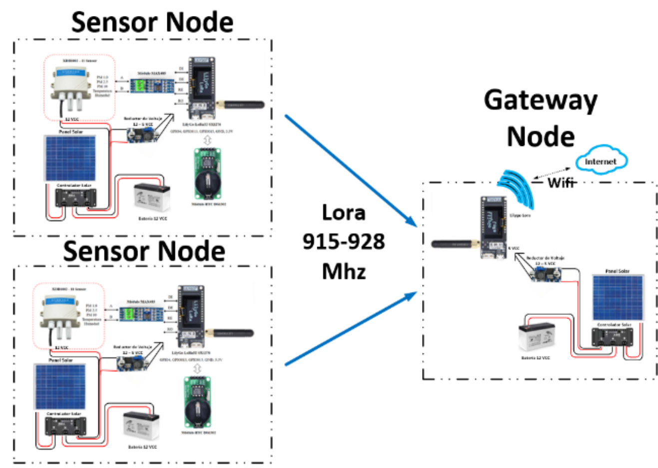

Fig.6 Network Topology – PTM (point to multi point).

c) Power and physical protection subsystem: The power supply is based on photovoltaic systems, which consist of a 10Wp solar panel and a 12V/7Ah battery sized to ensure continuous operation for both types of nodes. For physical protection, an IP65 enclosure was chosen, ideal for rainy environments such as Cusco. Fig. 7 shows the detail of a sensor node assembly, while Fig.8 shows the final implementation result.

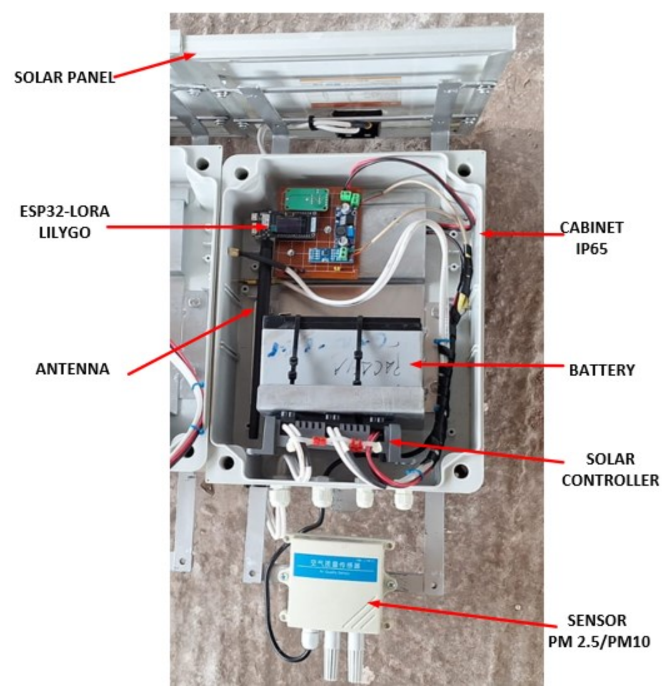

Fig.7 Internal components of the sensor node.

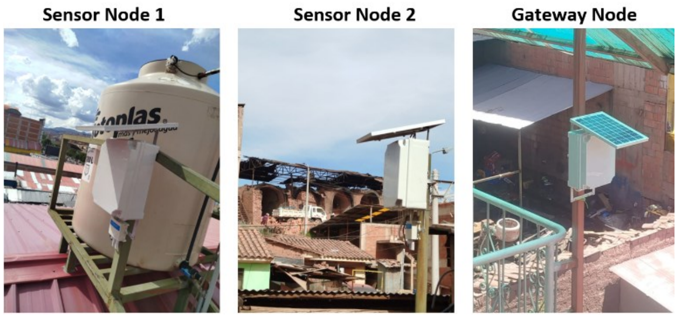

Fig.8 Network Topology – PTM (Point to multipoint).

According to the photovoltaic system sizing criteria in [9], an autonomy time estimation was performed, considering consumption and the worst level of solar radiation in Cusco, taking into account the current values of the available elements, to later perform an upgrade of the solution. An approximate consumption of 2 W-h and 4 W-h was obtained, respectively, from which an operating autonomy on the order of 14 and 30 hours is inferred (see Fig. 9). This result raises the need to evaluate whether such a time margin is sufficient to ensure power supply, particularly during periods without direct solar radiation availability.

Load	Details	Qty	Hours	Power (watt)	Constant	W-h/day	Subtotal Watts
Nodo Gateway	Voltaje: 12 Corriente: 0.154 A	1	24	1.85	1	44	1.848
							1.848
					Total de energía necesaria en un día	**44**	W-h/día
					Pérdidas	**1.2**	%
					Total energía necesaria	**53.2**	W-h/día

Numero de paneles	**1**		**Numero de Baterías**	**1**	
Potencia pico del módulo	10 Wp		Capacidad de una batería	7 Ah	
Radiación a 1000w/m2(peor mes) en horas	4.75 h/día		Voltaje de batería	12 V	
Total energía generada	48 W-h/día		Capacidad banco de batería	84 W-h	
Relación carga/descarga	**0.89**		Profundidad de descarga	0.8	
			días de autonomía	**1.3**	**30 H**

Load	Details	Qty	Hours	Power (watt)	Constant	W-h/day	Subtotal Watts
Nodo Sensor	Voltaje: 12 Corriente: 0.334 A	1	24	4.01	1	96	4.008
							4.008
					Total de energía necesaria en un día	**96**	W-h/día
					Pérdidas	**1.2**	%
					Total energía necesaria	**115.4**	W-h/día

Numero de paneles	**1**		**Numero de Baterías**	**1**	
Potencia pico del módulo	10 Wp		Capacidad de una batería	7 Ah	
Radiación a 1000w/m2(peor mes) en horas	4.75 h/día		Voltaje de batería	12 V	
Total energía generada	48 W-h/día		Capacidad banco de batería	84 W-h	
Relación carga/descarga	**0.41**		Profundidad de descarga	0.8	
			días de autonomía	**0.6**	**14 H**

Fig.9 Photovoltaic power sizing.

According to the estimate, although it is possible to guarantee more than 12 hours of autonomy, the battery charge/discharge ratio does not reach the recommended values according to [10], which suggests a value greater than 1.3. Consequently, an upgrade to use 12 Wp and 25 Wp solar panels is considered necessary in order to ensure an adequate charging process for the solution, guarantee continuous and reliable operation of the system, and prevent interruption of measurements.

d) Visualization subsystem: For this stage, it is important to mention that the gateway node plays an important role as a bridge, receiving LoRa frames and retransmitting them via Wi-Fi using HTTP POST requests to a server hosted on GCP, where the data are finally processed for subsequent visualization. The application layer is hosted on Google Cloud Platform (GCP), where time-series storage and information visualization are managed through a dashboard. The backend infrastructure is deployed on a virtual machine with Ubuntu within a Virtual Private Cloud (VPC) in GCP, which ensures system security and scalability. Moreover, the software solution was implemented using Docker containers to orchestrate three main services, as shown in Fig.10.

- Nginx: Acts as a reverse proxy and web server, managing HTTP/HTTPS requests and providing an SSL/TLS security layer.
- InfluxDB: A time-series optimized database responsible for storing historical sensor records with high write and query efficiency.

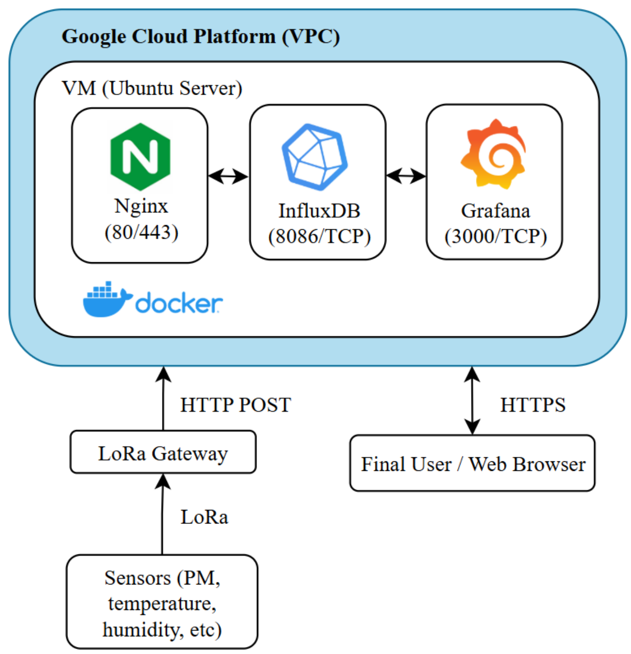

Fig.10 Cloud Architecture of the Solution

- Grafana: Used as a visualization tool connected to InfluxDB, enabling the generation of dynamic dashboards for system monitoring. This platform facilitated the presentation of sensor node data in a georeferenced manner. Fig.11, shows the platform used for information visualization.

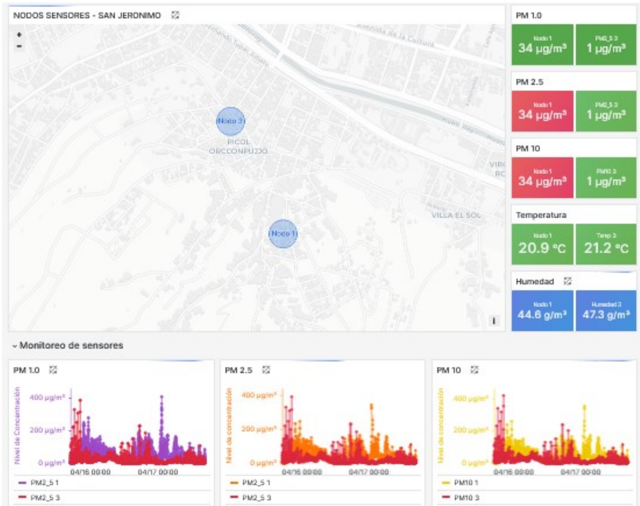

Fig.11 Proposed monitoring panel for node 1 and 2 in the San Jerónimo district.

IV. RESULTS AND DISCUSSION

System validation was performed in a real environment in the San Jerónimo district, evaluating three critical parameters: radiofrequency coverage, network performance (PDR), and energy autonomy.

A. Coverage and Link Quality Analysis

Field tests were carried out to contrast the theoretical link budget with real propagation in a semi-urban environment. Using the 915–928 MHz band, effective coverage was validated within a radius of up to 2.39 km from the gateway. This means that satisfactory transmissions could be carried out up to this distance. Fig.12 illustrates the route taken by the Gateway and the RSSI (Received Signal Strength Indicator) level received by node 2 (shown as a heat map); these measurements ranged between -95 dBm and -120 dBm. Although these values are lower than the theoretical free-space path loss (FSPL) estimate of -77 dBm for 2.5 km, communication remained stable thanks to the robustness of LoRa modulation and sensitivity levels below -130 dBm.

The Signal-to-Noise Ratio (SNR) analysis showed consistently positive values (> 1.5 dB) even at the farthest nodes, confirming that the signal is demodulable above the noise floor.

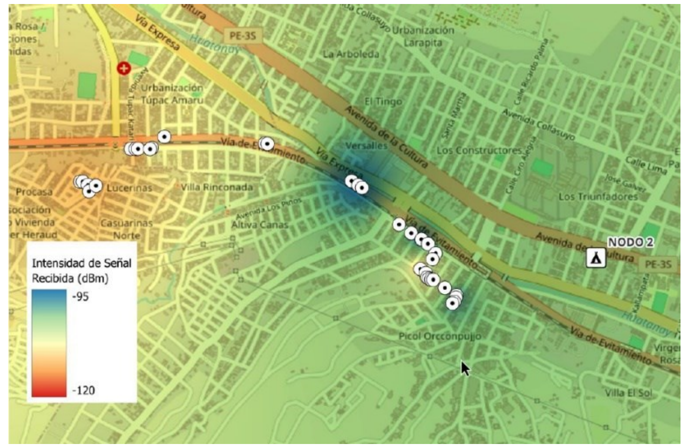

Fig.12 RSSI heat map for Node 2 coverage.

B. Network Performance

At an initial stage, the reliability of data transport was evaluated using the Packet Delivery Ratio (PDR), recorded during a continuous high-frequency transmission window with 10-second intervals over the course of one hour. According to the results presented in Table II, the node closest to the gateway achieved a PDR of 79.77%; the observed losses are mainly attributed to saturation of the gateway buffer caused by the asynchronous processing of incoming packets. In turn, the farthest node showed a PDR of 72.85%, a value that reflects the combined effect of signal attenuation with distance and the occurrence of possible collisions in the communication channel. The overall average PDR obtained was 76.35%.

TABLE II
NETWORK PERFORMANCE SUMMARY (PDR)

Sensor Node	Distance (m)	Received packets	Lost packets	Expected packets	PDR %
Node 1 (far)	800	279	104	383	72.9%
Node 2 (near)	10	280	71	351	79.8%
Average	-	-	-	-	76.35%

In a second improvement stage, changes were implemented to optimize network performance and increase the reliability of the Packet Delivery Ratio (PDR). To this end, a burst transmission scheme was introduced for one of the sensor nodes, which sends three consecutive packets per minute with the same content and sequence number, generating multiple delivery attempts (see Fig. 13). Likewise, two metrics were defined: the real PDR, which considers all transmitted packets (including retries), and the effective PDR, which counts a successful delivery if at least one of the attempts is received.

Additionally, the infrastructure was optimized by relocating the gateway to less than 10 m from the Wi-Fi access point and using a higher-gain Yagi antenna, thereby increasing the EIRP and consequently the received signal level.

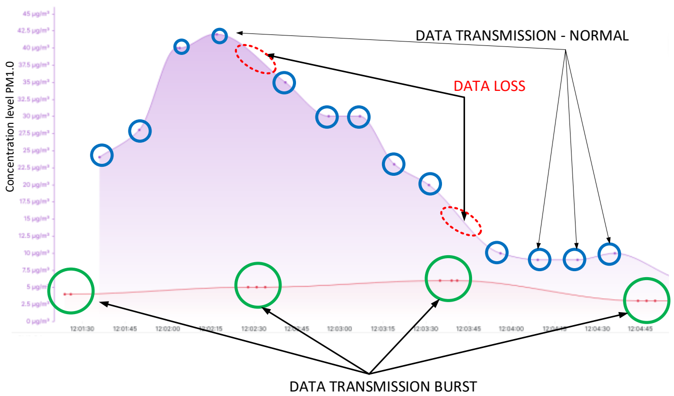

Fig.13 System transmission schemes, burts and data loss.

Similarly, Table III presents a comparison of the PDR for the nodes, using data collected over two days. For this analysis, the most distant node maintained the original configuration without retries, while the node closest to the gateway operated with the burst transmission scheme (as shown in Fig. 13), making it possible to highlight the improvement in network reliability. The effectiveness of the received data was confirmed: for the closest node, the percentage of successfully received data increased from 92.2% to 100%, thus validating this technique. These results are described in greater detail in Table III.

TABLE III
NETWORK PERFORMANCE SUMMARY (PDR)

Sensor Node	Real			Efective		
	Received packets	Lost packets	PDR (%)	Received packets	Lost packets	PDR (%)
Nodo (far)	11752	2134	84.6%	11752	583	84.6%
Nodo (near)	7070	583	92.2%	2501	0	100%
Average	-	-	88.4%	-	-	92.3%

Finally, the global average effective PDR is 92.3%, while the global real PDR is 84.6%. These results are considered acceptable for monitoring environmental trends, as they exceed the 80% threshold.

C. Particulate matter measurements

As part of the measurements carried out using the XDB1002-11 sensor, the PM10 monitoring reveals marked differences between the two locations. The station located near the kilns (red line) records peaks above 800 µg/m³, far exceeding WHO standards, whereas the station farther away in the urban area (blue line) shows lower and more stable concentrations, indicating a significant attenuation of the pollutant with distance. Nevertheless, high episodes still occur, confirming that industrial emissions continue to affect the air quality of the surrounding urban area. See Fig. 14

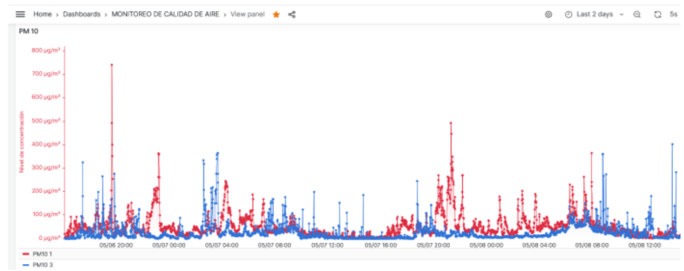

Fig.14 Measurements PM 10.

In turn, the PM2.5 monitoring shows that proximity to the kilns results in substantially higher concentrations. The orange series (near the kilns) exhibits peaks above 300 µg/m³, whereas the green series (located more than 500 m away in an urban area) records considerably lower values, generally below 200 µg/m³. See Fig. 15.

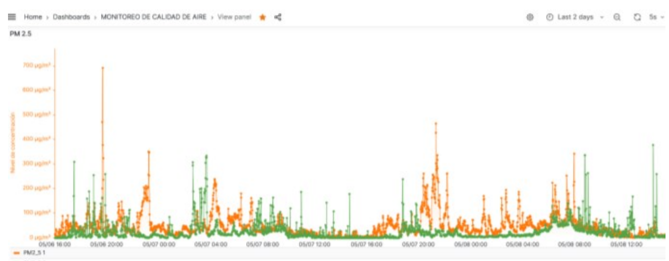

Fig.15 Measurements PM 2.5.

The temporal synchronization of the peaks in both series confirms the kilns as the main source of pollution. Although attenuation with distance is evident for both pollutants, PM2.5 particles show a greater capacity for dispersion and transport than PM10, affecting a larger urban area and maintaining elevated levels even 500 m from the emission source. The results show that exposure decreases considerably with distance; however, the impact of industrial emissions on air quality remains significant in the surrounding urban environment.

V. CONCLUSIONS

A LoRa-based IoT network for monitoring particulate matter (PM2.5 and PM10) was successfully designed and implemented in San Jerónimo, Cusco. The proposed architecture validated the integration of the industrial XDB1002-11 sensor with ESP32 microcontrollers via the Modbus-RTU protocol, ensuring accurate data acquisition and real-time visualization through a scalable cloud platform based on InfluxDB and Grafana.

Field tests in a semi-urban environment confirmed the robustness of LoRa modulation in the 915–928 MHz band, achieving stable links up to 2.39 km with RSSI levels between −95 dBm and −120 dBm and positive SNR values, thus validating its suitability for distributed environmental monitoring in obstructed scenarios. In the initial stage, the average PDR obtained (76.35%) was below the desirable threshold (≥ 80%) for applications involving continuous trend tracking, highlighting the need for optimization. However, the implementation of a burst transmission scheme, the relocation of the gateway, and the use of a higher-gain antenna increased the average effective PDR to 92.3%, significantly surpassing the minimum threshold and demonstrating the effectiveness of the optimization strategies implemented.

From an energy perspective, the photovoltaic sizing ensured autonomies on the order of 14 to 30 hours, sufficient to validate system operation, although the battery charge/discharge ratio remained below recommended values, which could compromise sustained operation under adverse solar-radiation conditions. Consequently, optimizing the energy subsystem is identified as a priority line of improvement, whether by increasing the peak power of the panels, adjusting the transmission cycles, or incorporating more efficient energy-management strategies; this should be regarded as future improvement work.

The analysis of particulate-matter measurements revealed significant differences between the monitoring stations. Proximity to the artisanal kilns produces critical concentrations that far exceed WHO standards, with peaks above 800 µg/m³ for PM10 and 300 µg/m³ for PM2.5. Although a considerable attenuation with distance is evident, industrial emissions continue to affect air quality in the surrounding urban environment, with PM2.5 particles showing a greater capacity for dispersion and transport than PM10.

Overall, the results show that the proposed solution is a tool capable of strengthening local air-quality management and supporting decision-making regarding pollution generated by artisanal brick kilns, by facilitating the continuous, reliable, and accessible generation of environmental information. The successful validation of the system after the implemented optimizations confirms the technical and operational feasibility of LoRa networks for environmental-monitoring applications in rural and semi-urban contexts in developing countries.

ACKNOWLEDGMENT

The authors would like to thank the Grupo de Telecomunicaciones Rurales of the Pontificia Universidad Católica del Perú (PUCP) and Enertec Ingenieros y Servicios S.A.C. for their support.

REFERENCES

[1] W. H. Organization, «WHO global air quality guidelines: particulate matter (PM2.5 and PM10), ozone, nitrogen dioxide, sulfur dioxide and carbon monoxide,» 2021.

[2] J. Wharton, A. Zamalloa, B. W. Amanda Olarte y I. Miranda, «A Comprehensive Assessment of PM2.5 and PM10 Pollution in Cusco, Peru: Spatiotemporal Analysis and Development of the First Predictive Model (2017–2020),» Cusco, 2025.

[3] MINAM, «DECRETO SUPREMO Nº 003-2017-MINAM: Aprueban Estándares de Calidad Ambiental (ECA) para Aire y establecen Disposiciones Complementarias».

[4] W. A. Jabbar y T. Subramaniam, «LoRaWAN-Based IoT System Implementation for Long-Range Outdoor Air Quality Monitoring,» 2022.

[5] S. García, D. F. Larios y J. Barbancho, «Heterogeneous LoRa-Based Wireless Multimedia Sensor Network Multiprocessor Platform for Environmental Monitoring,» 2019.

[6] L. República, «Salud de cusqueños en riesgo porque Municipalidad de San Jerónimo no cierra ladrilleras ilegales que contaminan el aire,» La República, 2024. [En línea]. Available: https://larepublica.pe/sociedad/2024/10/20/cusco-salud-de-ciudadanos-en-riesgo-porque-municipalidad-de-san-jeronimo-no-cierra-ladrilleras-ilegales-que-contaminan-el-aire-272660. [Último acceso: 2026].

[7] A. I. &. Z. P. S. Ali, «Development and performance analysis of a ZigBee and LoRa-based smart building sensor network. Electronics,» *Internet of Things for Smart Buildings ,* 2022.

[8] Shenzhen Zhongdian Metrology and Testing Technology Co., Ltd., "校准证书 / Calibration Certificate No. ZD202312111681 for PM sensor SN-PM (used in XDB1002-11 air quality transmitter)," Shenzhen, China, Dec. 11, 2023

[9] L. RAMOS y D. Auccapuri, «Development of 4G base station for rural areas based on LimeSDR,» 2025.

[10] D. Espinoza . et al., Redes inalámbricas para zonas rurales. Lima, Perú: Editorial Pontificia Universidad Católica del Perú, 2008, ISBN 978-9972-42-843-2